

# Two-stage superconducting-quantum-interference-device amplifier in a high-Q gravitational wave transducer

Gregory M. Harry<sup>a)</sup>, Insik Jin, Ho Jung Paik, Thomas R. Stevenson<sup>b)</sup> , and  
Frederick C. Wellstood

*Center for Superconductivity Research, Department of Physics, University of Maryland,  
College Park, Maryland 20742*

(November 26, 2024)

## Abstract

We report on the total noise from an inductive motion transducer for a gravitational-wave antenna. The transducer uses a two-stage SQUID amplifier and has a noise temperature of 1.1 mK, of which 0.70 mK is due to back-action noise from the superconducting quantum interference device (SQUID) chip. The total noise includes thermal noise from the transducer mass, which has a measured  $Q$  of  $2.60 \times 10^6$ . The noise temperature exceeds the expected value of  $3.5 \mu\text{K}$  by a factor of 200, primarily due to voltage noise at the input of the SQUID. Noise from flux trapped on the chip is found to be the most likely cause.

Typeset using REVTEX

---

<sup>a)</sup>Present address: Department of Physics, Syracuse University, Syracuse, New York 13244-1130

<sup>b)</sup>Present address: Department of Applied Physics, Yale University, PO Box 208284, New Haven, Connecticut 06520-8284

Detection of gravitational waves from astronomical sources requires extremely low noise antennas and amplifiers [1]. The dominant noise source is the first stage electrical amplifier, which has typically been made from a superconducting quantum interference device (SQUID). Our previous work on gravitational wave transducers using a commercial SQUID from Quantum Design of San Diego California found a noise temperature of 3.9 mK, with 1.2 mK attributed to SQUID back-action noise [2]. Here we report noise measurements for an integrated two-SQUID system in which one SQUID amplifies the output of another. We use the interaction between the SQUID input and the high-Q transducer circuit to distinguish different noise sources internal to the SQUIDs.

The first-stage SQUID is used as an electrical amplifier and immediately follows the transducer, which is connected to the gravitational-wave antenna. The transducer used for these measurements was a Paik-style [3], inductive, resonant mass. Figure 1(a) shows a schematic of the antenna with a transducer mass. There are two coils of superconducting wire on either side of the transducer's proof mass, as shown in Fig. 1(b). Conservation of magnetic flux in a superconducting circuit requires that persistent current stored in these coils changes with inductance. This signal current is shunted to the transformer with primary  $L_{t1}$ . The secondary,  $L_{t2}$ , of this transformer is connected to the input of the SQUID chip.

The transducer was made from a round plate of niobium out of which circular grooves were milled on both faces, defining a central mass. The remaining thin niobium annulus acts as the mechanical spring connecting the central proof mass to the case. The case would be bolted rigidly to the antenna during gravitational-wave searches. The proof mass was electropolished in an acid solution and was heat treated to 1500° C to improve the quality factor of the resonance. Two other niobium plates were then bolted to either side of the proof mass and contain the sensing coils  $L_1$  and  $L_2$ . Measurements revealed 10  $\mu\text{m}$  gaps between the coils and the proof mass at room temperature and 25  $\mu\text{m}$  gaps at the operating temperature of 4.2 K.

The SQUID amplifier was comprised of two SQUIDs, the first serving as a preamplifier for the second [4]. Both SQUIDs had junctions made from Nb-Al/AlO<sub>x</sub>-Nb trilayers and were

impedance matched to the transducer circuit using a 40:1, thin-film, on-chip transformer. The first SQUID was kept in a flux-locked loop by modulating the second SQUID with a 500 kHz square-wave signal. The demodulated signal was negatively fed back to the first SQUID to linearize the amplifier response. A second feedback loop was employed to keep the flux gain between the SQUIDs at a maximum [5] (see Figure 2). The additional loop modulated the second SQUID with a small amplitude flux signal at 8 kHz. This signal was demodulated at 16 kHz and the resulting low frequency signal was negatively fed back to the second SQUID. Using the second harmonic of the input signal as the source of the feedback flux made this loop sensitive to the second derivative of the inverse of the function

$$\Phi_2(\Phi_1) = \frac{G_\Phi}{2\pi} \sin\left\{\frac{2\pi}{\Phi_0}[\Phi_1 + \Phi_{B1}(t)]\right\} + \Phi_{B2}(t), \quad (1)$$

where  $\Phi_2$  is the flux in the second SQUID,  $\Phi_1$  is the flux in the first SQUID,  $G_\Phi$  is the maximal flux gain between the two SQUIDs,  $\Phi_0$  is the quantum of magnetic flux, and  $\Phi_{B1}(t)$  and  $\Phi_{B2}(t)$  are the (possibly time-varying) background fluxes in the first and second SQUID, respectively. This process is equivalent to maximizing the flux gain  $d\Phi_2/d\Phi_1$  by shifting the background fluxes. Determining and then maintaining this maximized flux gain against changing an external background flux  $\Phi_{B2}(t)$  is necessary to minimize the effect of noise from both SQUIDs.

To make noise measurements, the SQUID amplifier was connected to the transducer (the transducer was not attached to an antenna in these experiments but was instead suspended from a vibration isolator). A current of 6.5025 A was stored in the two coils surrounding the proof mass. The noise was recorded as voltage across the feedback resistor  $R_{fb}$ . Figure 3 shows the resulting root-mean-square flux noise spectrum in a 62.5 Hz bandwidth around the transducer resonance at 892 Hz. We use the observed contrast between constructive and destructive interference between correlated noise above and below the transducer resonance frequency, evident in Fig. 3, to make qualitative and quantitative inferences about the magnitude and source of back-action noise.

Two sources of noise were expected to dominate the total noise: additive noise from the

SQUID amplifier and thermal force noise from dissipation in the proof mass. The expected signal-to-noise ratio density,  $r(\omega)$ , can be written [6],

$$r(\omega) = \frac{2\Re[Z_n]\mu\omega^2}{k_B T_n |k - \mu\omega^2 + j\omega Z_n|^2}, \quad (2)$$

where  $Z_n$  is the mechanical noise impedance,  $\mu$  is the reduced mass of the proof mass and case mass,  $k$  is the spring constant between the proof mass and the case,  $k_B$  is Boltzmann's constant, and  $T_n$  is the noise temperature. This quantity  $r(\omega)$  represents the sensitivity of the transducer per unit energy deposited in the transducer resonance by a signal. A more complete discussion of its derivation and use can be found in [6] and [7].

After calibrating the transducer response to a mechanical signal, we used Eq. 2 to describe the total noise in terms of a noise temperature  $T_n$  and a complex noise impedance  $Z_n$ . The values of  $T_n$  and  $Z_n$  describe the total force and velocity noises and their correlation and can be found from fitting the noise data to Eq. 2. We found from this fit

$$T_n = 1.08 \times 10^{-3} \text{ K}, \quad (3)$$

$$Z_n = (16.9 + 4.24 j) \text{ kg/s}. \quad (4)$$

The double-sided spectral density of force noise, velocity noise, and their correlation can then be obtained from these parameters [6]. Through additional calibration measurements [7], we were able to characterize the electromechanical circuit parameters in the transducer and SQUID chip to allow us to quantitatively relate  $T_n$  and  $Z_n$  to various possible mechanical and electrical noise sources internal to the transducer and SQUIDs.

The back-action noise due to the SQUID was determined by subtracting the thermal force noise from the total force noise observed. The thermal noise arises from the dissipation of the transducer resonance. The magnitude of the thermal force noise can be predicted using the fluctuation-dissipation theorem and the measured exponential decay time of the resonance. The Q for this mode is measured directly from the damped oscillation and was found to be

$$Q = 2.60 \times 10^6, \quad (5)$$

which includes contributions from the mechanical spring and the electrical spring created by the stored currents. This  $Q$ -value has been corrected for cold damping produced by the SQUID feedback loop [2] so that it gives the passive dissipation in thermal equilibrium at the transducer temperature. By studying the dependence of  $Q$  on stored current, the total  $Q$  could be broken down into mechanical and electrical components [3]:

$$Q_m = 3.15 \times 10^6, \quad (6)$$

$$Q_e = 2.52 \times 10^5. \quad (7)$$

The thermal force noise can be found using the total  $Q$  from

$$S_f = 2k_B T \frac{\omega_0 \mu}{Q}, \quad (8)$$

where  $T$  is the measured physical temperature,  $\omega_0$  is the resonance frequency,  $\mu$  is the reduced mass of the proof mass and the case, and  $Q$  is the measured, passive  $Q$  of the resonance. After subtracting this thermal noise, the noise temperature of the SQUID amplifier was found to be

$$T_s = 6.99 \times 10^{-4} \text{ K}. \quad (9)$$

Using a circuit model [2,7] for the transducer and SQUID input circuit, we calculated the SQUID's electrical noise impedance:

$$Z_s = (5.9 \times 10^{-3} - 8.9 \times 10^{-6} j) \Omega. \quad (10)$$

We also performed tests on the SQUID without the transducer attached. The input port was left open-circuited and the entire SQUID chip was contained in a niobium box. The SQUID's energy sensitivity in this configuration was  $9.22 \times 10^{-6}$  K. We note that with only one port on the amplifier available, the noise can only be expressed as a single number and a true noise temperature can not be calculated.

We used the method of Clarke, Tesche, and Giffard [8], as extended by Martinis and Clarke [9], to calculate the minimum or true noise temperature of the SQUID expected from the Johnson noise of its shunt resistors:

$$T_{\text{CTG}} = 3.5 \times 10^{-6} \text{ K.} \quad (11)$$

Table I presents the Clarke-Tesche-Giffard (CTG) predictions for each noise component as well as the experimental results. The data is presented as both the experimental result and as a minimum limit derived from the data. These limits come from using the observed high/low frequency asymmetry seen in the noise spectrum while assuming the thermal noise is large enough that an accurate force noise subtraction cannot be done. The voltage noise and current noise must be at least as large as this limiting case.

The measured noise temperature is a factor of 200 above the expected noise of  $T_{\text{CTG}}$ , thereby reducing the sensitivity of the transducer through Eq. 2. This noise is almost exclusively due to voltage noise at the input of the SQUID as the excess noise is observable only when the SQUID is coupled to the high-Q transducer. We examined possible explanations for this excess voltage noise. Flux creep in the large sensing coils  $L_1$  and  $L_2$  (see Figure 1 (b)) was eliminated as a possible source based on the predicted signature of the two noise components. Noise from a varying magnitude RF signal was also considered [2] but was rejected because we expect an accompanying large current noise, which was not observed. Noise from flux lines moving between pinning sites in the on-chip transformer  $L_{s4}$  was modeled using the method of Ferrari *et al.* [10]. We found that the product

$$nS_r = 9.1 \times 10^{-9} \text{ Hz}^{-1}, \quad (12)$$

where  $n$  is the flux vortex density and  $S_r$  is the spectral density of the flux's radial motion, would give rise to the observed voltage noise. This same  $nS_r$  would predict values of

$$S_I(\omega_0 L)/k_B = 1.8 \pm 0.7 \text{ } \mu\text{K}, \quad (13)$$

$$|S_{VI}|/k_B = 80 \pm 30 \text{ } \mu\text{K}. \quad (14)$$

The predicted value of the current noise is below the CTG value, so on-chip flux noise would not be significant. The correlation noise agrees within the error bars with the experimental limit in Table I.

While the back-action noise we observe would allow only modest sensitivity improvement for detectors operating at 4 K [1], the potential for millikelvin detectors [11,12] may be better. We were unable to measure the SQUID in a transducer at millikelvin temperatures, but separate noise measurements on a similar chip in a dilution refrigerator [13,14] indicate flux motion noise may be much less at 90 mK, depending on the source of the flux. Our SQUID is being considered for use in a multimode transducer on the ALLEGRO detector [1] and, with further research, it may be possible to improve the 4 K performance by using a heater to expel flux.

This work was supported by grant PHY93-12229 from the National Science Foundation and by the Gravitational Wave Lab at Louisiana State University.

## TABLES

TABLE I. Voltage and current noise at the input of the first SQUID. The three columns represent the experimentally determined values, the minimum experimental limits, and the values predicted from Clarke-Tesche-Giffard theory. All noise values are presented in temperature units using the inductance of the pickup coils as expressed through the two transformers,  $L = 740$  pH.

Parameter	Experimental Value	Limit	CTG Value
$S_V/\omega_0 L k_B$	3.3 mK	400 $\mu$ K	0.8 $\mu$ K
$S_I(\omega_0 L/k_B)$	490 $\mu$ K	20 $\mu$ K	50 $\mu$ K
$-\Im[S_{VI}]/k_B$	1.1 mK	100 $\mu$ K	5.3 $\mu$ K

## FIGURES

FIG. 1. (a) Mechanical model of antenna with transducer mass. The equivalent mass of the antenna,  $M_1$ , is connected by a spring with constant  $k_1 = M_1\omega_0^2$  to mechanical ground and the antenna is connected to the proof mass,  $M_2$ , by a spring with constant  $k_2 = M_2\omega_0^2$ . The force from the gravitational wave,  $F$ , acts between mechanical ground and the antenna mass. (b) Circuit diagram of the transducer. The proof mass can move between the two pickup coils,  $L_1$  and  $L_2$ . The signal current from this motion passes through two transformers to the first SQUID. All of the wiring in the transducer circuit is superconducting.

FIG. 2. Dual feedback loops used to control the two-SQUID system. The flux-locking loop is at 500 kHz. The modulation is sent to the second SQUID and the low frequency feedback is sent to the first SQUID. The loop to maximize the flux gain modulates the second SQUID at 8 kHz, but is demodulated at 16 kHz.

FIG. 3. Noise spectral density near the transducer resonance expressed as flux in the first SQUID. The asymmetry in the peak indicates an excess of back-action noise.

## REFERENCES

- [1] Z. K. Geng, W. O. Hamilton, W. W. Johnson, E. Mauceli, S. Merkowitz, A. Morse, N. Solomonson, in *First Edoardo Amaldi Conference on Gravitational Wave Experiments*, edited by E. Coccia, G. Pizzella, and F. Ronga (World Scientific, Singapore, 1995) 128-135.
- [2] T. R. Stevenson and H. J. Haucke, in *First Edoardo Amaldi Conference on Gravitational Wave Experiments*, edited by E. Coccia, G. Pizzella, and F. Ronga (World Scientific, Singapore, 1995) 390-397.
- [3] H. J. Paik, J. Appl. Phys. **47**, 1168 (1976).
- [4] I. Jin, Ph.D. thesis, University of Maryland, College Park, 1997.
- [5] T. R. Stevenson, oral presentation at Fourteenth International Conference on General Relativity and Gravitation (Florence Italy, 1995).
- [6] J. C. Price, Phys. Rev. D **36**, 3555 (1987).
- [7] G. Harry, Ph.D. thesis, University of Maryland, College Park, 1999.
- [8] J. Clarke, C. D. Tesche, and R. P. Giffard, J. Low Temp. Phys. **37**, 405 (1979).
- [9] J. M. Martinis and J. Clarke, J. Low Temp. Phys. **61**, 227 (1985).
- [10] M. J. Ferrari, J. J. Kingston, F. C. Wellstood, and J. Clarke, Appl. Phys. Lett. **58**, 1106 (1991).
- [11] M. Cerdonio, L. Franceschini, G. Fontana, R. Mezzena, S. Paoli, G. A. Prodi, S. Vitale, J. P. Zendri, M. Biasotto, M. Lollo, F. Bronzini, R. Macchietto, G. Maron, A. Ortolan, M. Strollo, G. Vedovato, M. Bonaldi, P. Falferi, E. Cavallini, P. L. Fortini, E. Montanari, L. Taffarello, A. Colombo, D. Pascoli, and B. Tiveron, in *First Edoardo Amaldi Conference on Gravitational Wave Experiments*, edited by E. Coccia, G. Pizzella, and F. Ronga (World Scientific, Singapore, 1995) 176-194.

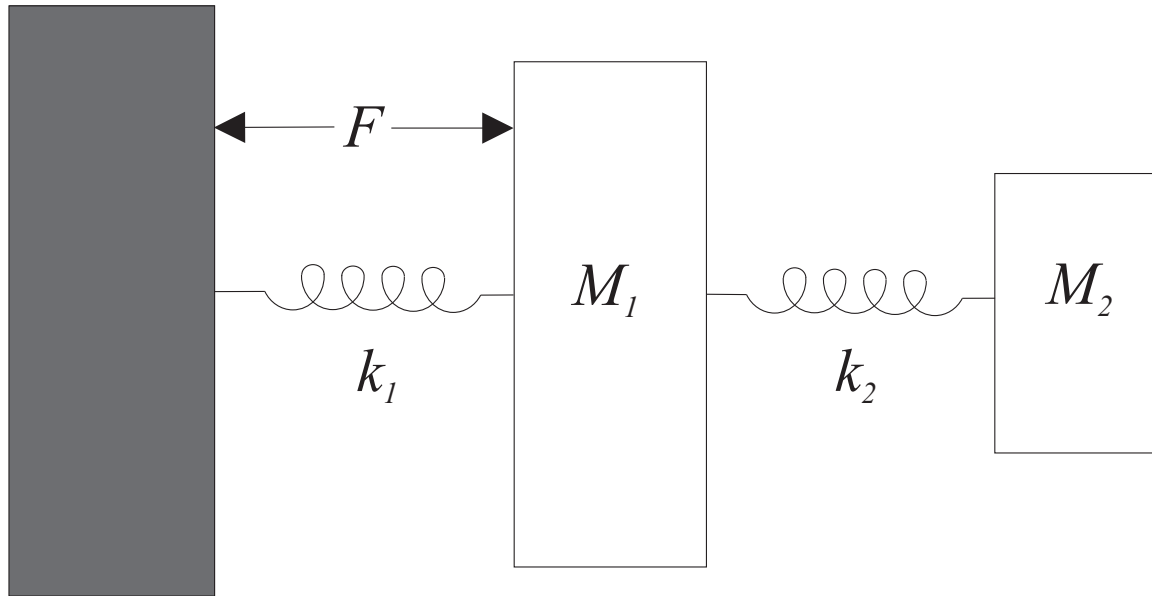
[12] P. Astone, M. Bassan, P. Bonifazi, P. Carelli, E. Coccia, C. Cosmelli, V. Fafone, S. Frasca, S. Marini, G. Mazzitelli, P. Modestino, I. Modena, A. Moleti, G.V. Pallottino, M. A. Papa, G. Pizzella, P. Rapagnani, F. Ricci, F. Ronga, R. Terenzi, M. Visco, and L. Votano, *Astroparticle Phys.* **7**, 231 (1997).

[13] I. Jin, A. Amar, T. R. Stevenson, F. C. Wellstood, A. Morse, and W. W. Johnson, *IEEE Trans. Appl. Supercond.* **7**, 2742 (1997).

[14] I. Jin, A. Amar, and F. C. Wellstood, *Appl. Phys. Lett.* **70**, 2186 (1997)

Figure 1 - G. M. Harry *et al.*

(a)



(b)

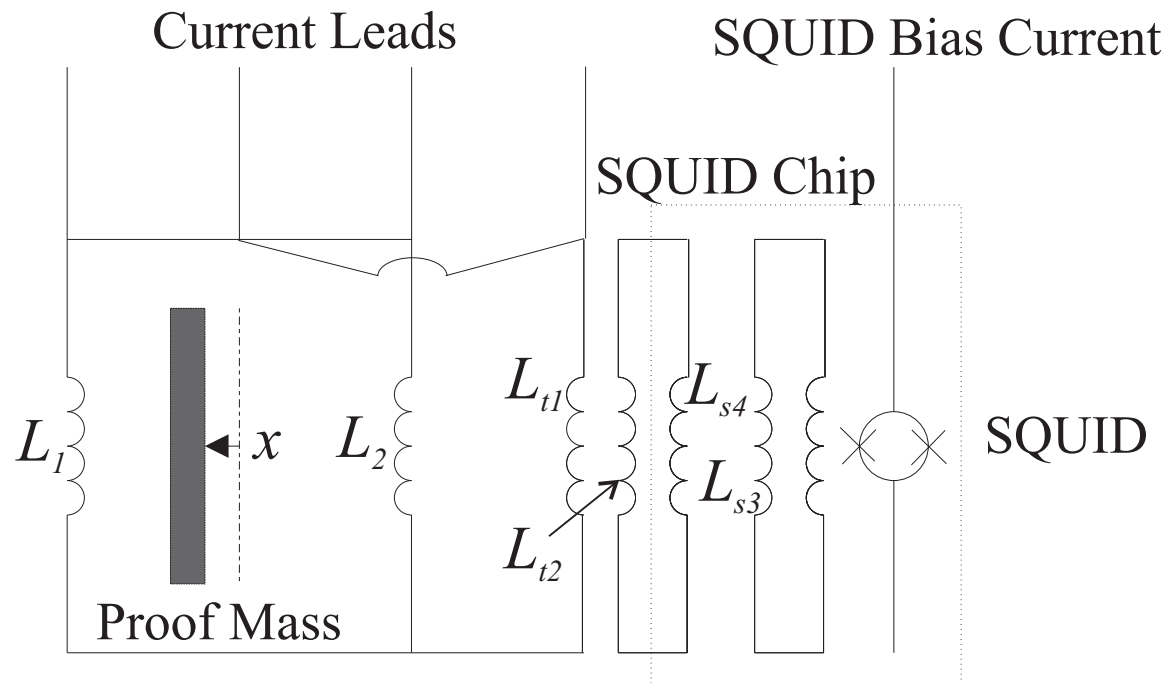


Figure 2 - G. M. Harry *et al.*

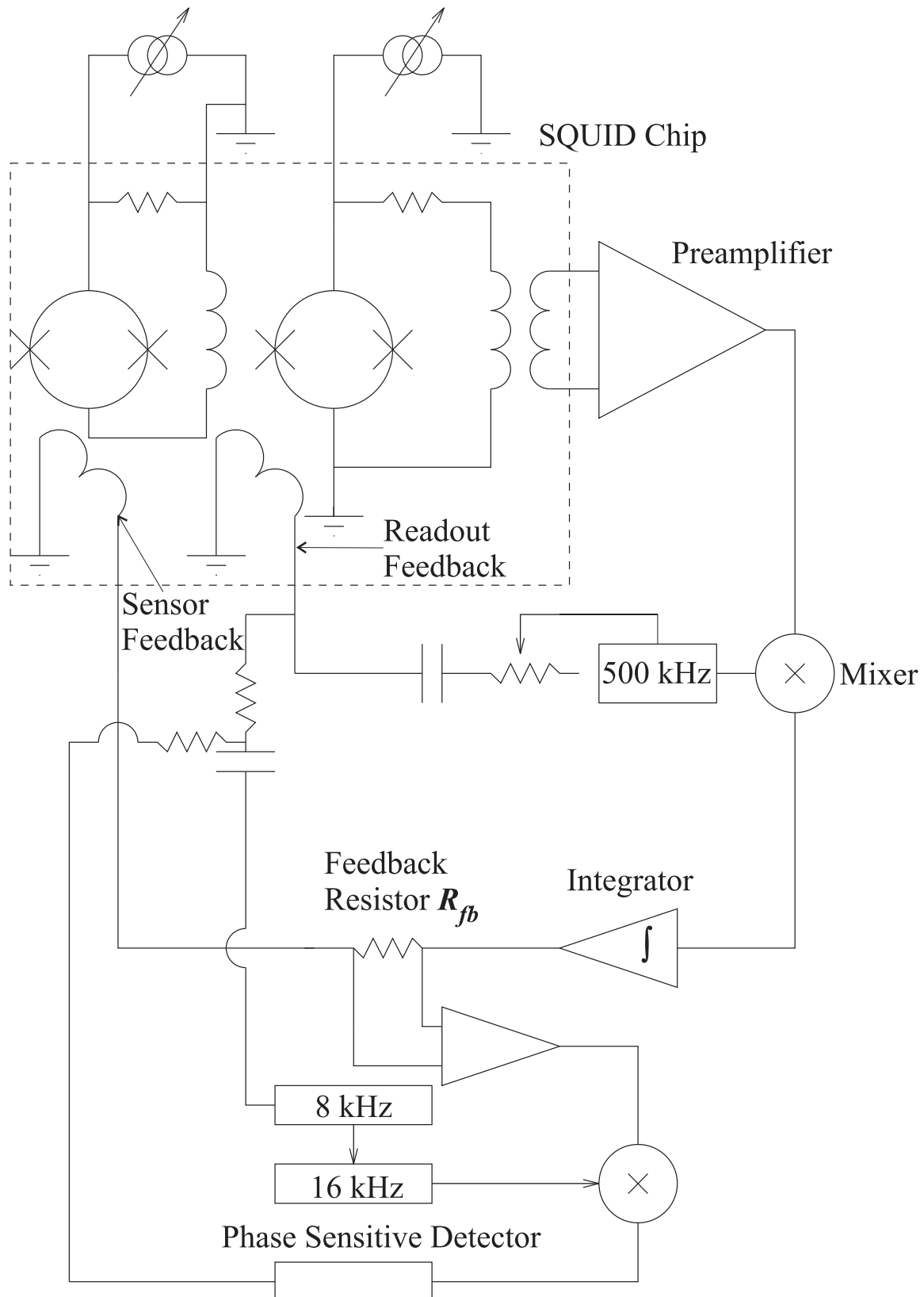


Figure 3 - G. M. Harry *et al.*

